LEAVE THIS PAGE BLANK
DO NOT DELETE THIS PAGE

From design to the fabrication of shellular funicular structures

Mostafa Akbari
Yao Lu
Masoud Akbarzadeh

Polyhedral Structures Laboratory, Stuart Weitzman School of Design, University of Pennsilvania

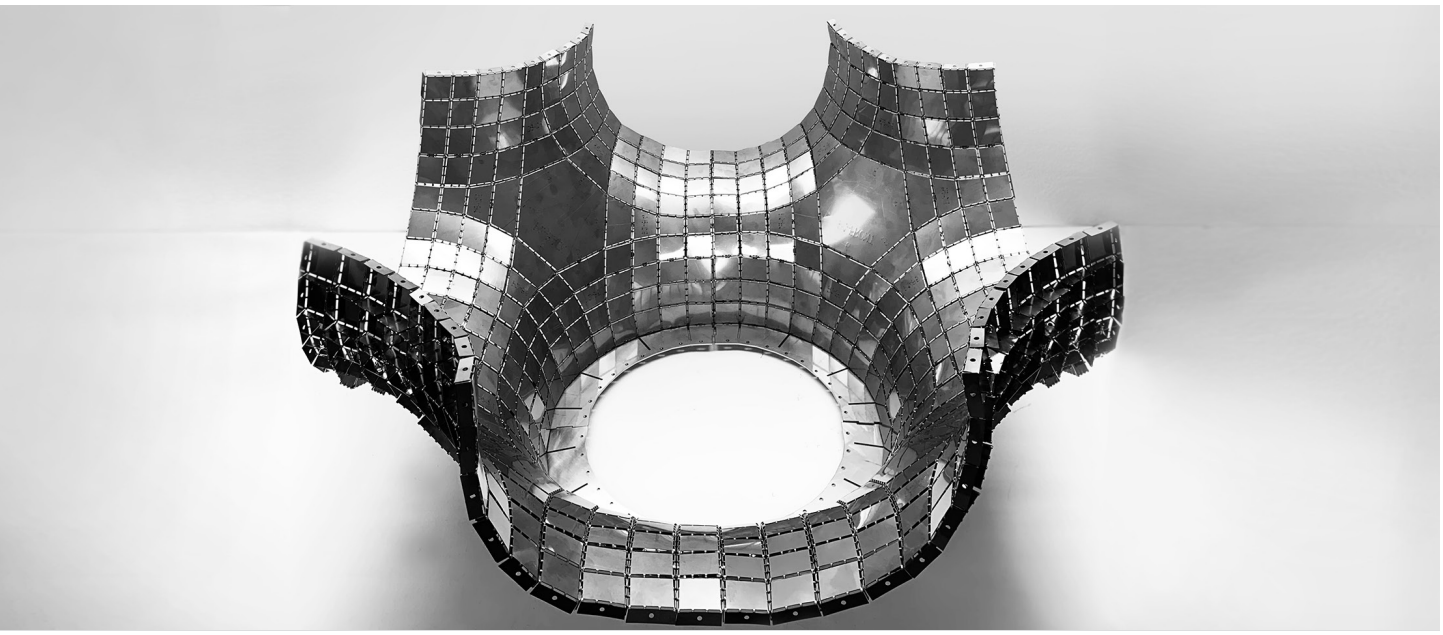

Hero image

ABSTRACT

Shellular Funicular Structures (SFSs) are single-layer, two-manifold structures with anticlastic curvature, designed in the context of graphic statics. They are considered as efficient structures applicable to many functions on different scales. Due to their complex geometry, design and fabrication of SFSs are quite challenging, limiting their application in large scales. Furthermore, designing these structures for a predefined boundary condition, control, and manipulation of their geometry are not easy tasks. Moreover, fabricating these geometries is mostly possible using additive manufacturing techniques, requiring a lot of supports in the printing process.

Cellular funicular structures (CFSs) as strut-based spatial structures can be easily designed and manipulated in the context of graphic statics. This paper introduces a computational algorithm for translating a Cellular Funicular Structure (CFS) to a Shellular Funicular Structure (SFS). Furthermore, it explains a fabrication method to build the structure out of a flat sheet of material using the origami/ kirigami technique as an ideal choice because of its accessibility, processibility, low cost, and applicability to large scales. The paper concludes by displaying a structure that is designed and fabricated using this technique.

Hero image : A shellular funicular structure fabricated using tuck-folding technique.

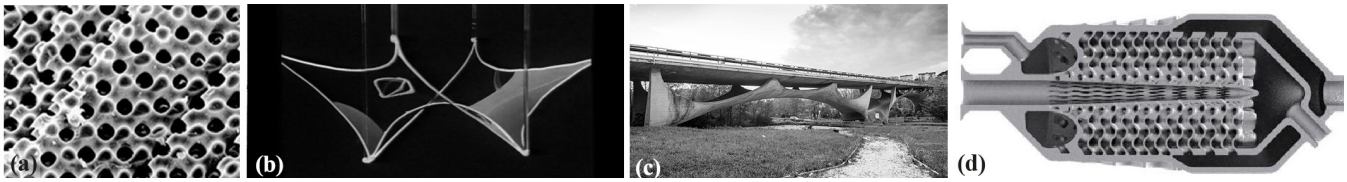

1 Shellular structures in nature, architecture and engineering; (a) cross-section through a sea urchin skeletal plate (Lai et al 2007), (b) Frei otto's physical form-finding using soap film (Otto 1970); (c) The bridge over the Basento by Sergio Musmeci (Canestrini, 1975); (d) Shellular structure's application in an aerospace turbine engine (Vlahinos and O'Hara 2020).

INTRODUCTION

Shellular structures

Shellular (shell cellular) structures are a category of cellular structures in nature, composed of single, continuous, smooth-curved shells (Figure 1). Their geometry includes surfaces filling the space with the least amount of material, called minimal surfaces (Meeks and Perez 2011; Han et al. 2015). Minimal surfaces in nature (e.g., soap film) have inspired many architects and engineers to design lightweight structures on large scales for many years (Otto 1970). Considering *k1* and *k2* as the principal curvatures of a minimal surface in each point, these surfaces have zero mean curvature ($H = (k1 + k2) / 2 = 0$) and negative Gaussian curvature ($G = k1 \times k2 < 0$) (Hilbert and Cohn-Vossen 1990). Recent studies show that due to their specific morphology and high surface-to-volume ratio, these structures have better mechanical performance compared to the other cellular structures (e.g., strut-based cellular structures) (Han et al. 2015; Han et al. 2017).

Graphic statics

Graphic statics as an intuitive method of structural design has been used to design and analyze structures for many years (Maxwell 1864, Rankine 1864; Culmann 1866; Cremona 1890; Beghini et al. 2013). This method allows the designer to design a structure by exploring its form and force simultaneously. Using reciprocal diagrams, one is able to control the internal flow of force and external loading scenario while designing the structure. Three-dimensional graphic statics (3DGS), as an extension of 2D graphic statics, enables the designer to design three-dimensional and axially loaded structures in equilibrium in which no bending occurs (Akbarzadeh 2016; McRobie 2016; Konstantatou et al. 2017; D'acunto et al. 2017; Akbarzadeh et al. 2021). In this method, there is a clear relation between the form and force diagrams as a pair of reciprocal diagrams linked through simple geometric constraints. In 3DGS, a closed polyhedron can represent the equilibrium of a three-dimensional node (Figure 2a). Each edge e_i or force f_i in the form diagram is perpendicular to the corresponding face $f_i^{\dagger}$ in the force diagram. The form diagram represents the geometry of the structure combined with the reaction forces and applied Figure loads (Figure 2, bottom), while the force diagram represents the equilibrium of internal and external forces (Figure 2, top).In this paper, the form is denoted by Γ and the force diagram by $\Gamma^{\dagger}$. Furthermore, all the topological elements related to the force diagram are denoted by † superscript.

Topologically speaking, these diagrams consist of vertices v_i, edges e_i, faces f_i, and cells c_i. Each vertex, edge, face, and cell ($v_i^{\dagger}$, $e_i^{\dagger}$, $f_i^{\dagger}$, $c_i^{\dagger}$) in the force diagram corresponds to a cell, face, edge, and vertex (v_i, e_i, f_i, c_i) in the form diagram (Figure 2) (Akbarzadeh, 2016). Since these diagrams are reciprocal and the faces of the force diagram (corresponding to the form diagram's edges) are planar, the form diagram's faces (corresponding to the force diagram's edges) are planar as well (Akbarzadeh, 2016).

A closed and convex force diagram signifies a compression/tension-only structure in equilibrium. Furthermore, the magnitude of the force f_i in each strut member in the form diagram is proportional to the area of the corresponding face $A(f_i)$ in the force diagram (Figure 2a) (Akbarzadeh, 2016). This theory can be simply proved based on the divergence theorem (Strokes, 1901). Based on this theory, the sum of all area-weighted normals of a polyhedron is zero. As a form-finding technique, subdividing the internal space of the force diagram results in a variety of topologically different structures, designed for a defined boundary condition and loading scenario (Figure 2) (Akbarzadeh 2016; Akbari et al. 2019). Adding thickness to each edge of these form diagrams proportional to the area of its corresponding face in the force diagram results in a strut-based cellular funicular structure (CFC) (Figure 2).

Increasing the number of subdivisions in the force diagram results in a form diagram with smaller edges and distributed forces in the members (Figure 2a-d and e-f). This increase can finally result in the edges with near zero-length, approximating a surface as a form diagram. Specific subdivision techniques in 3DGS can approximate surfaces with synclastic or anticlastic curvatures as form diagrams (Akbari et al. 2019).

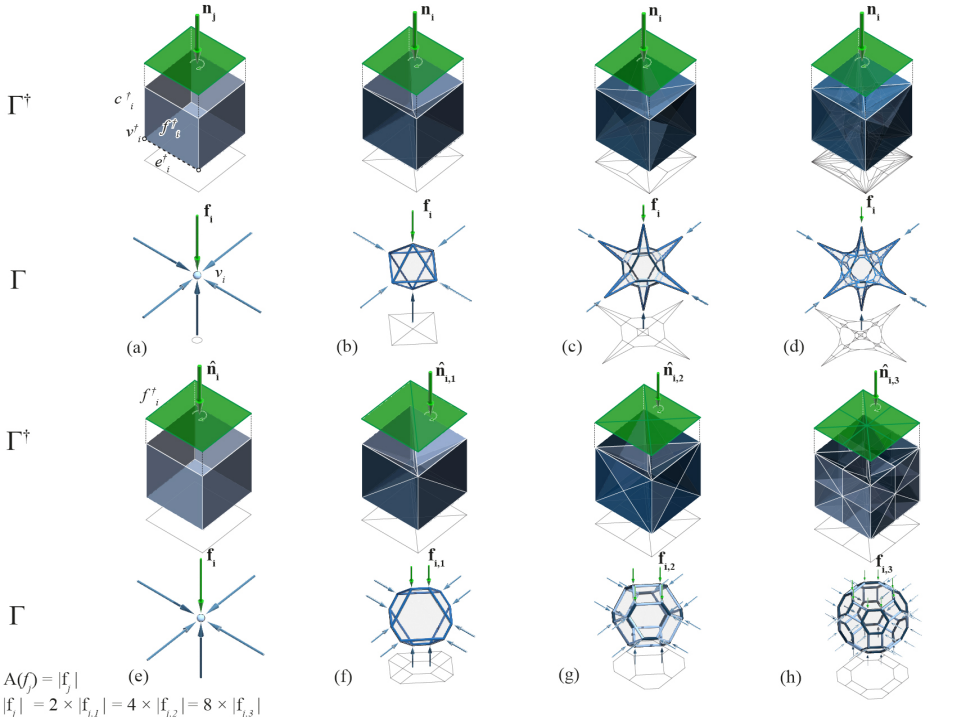

2 Different types of force diagram's subdivisions in 3DGS result in new form diagrams; (a), (e) a closed cube as a force diagram represents a node in equilibrium; (a-d) internal subdivision of a force diagram without subdividing the global faces; (e-h) subdivision of a force diagram while subdividing the external faces and extruding inside.

3 Different types of force diagram's Iterative subdivision of a tetrahedron as a force diagram approximates a discrete surface with anticlastic curvature (a-d) as the form diagram. Using this subdivision between specific labyrinth graphs, one can design a shellular funicular structure (e) and use the labyrinths as control handles to manipulate the structure (f).

4 Origamizing a polyhedral surface using tuck-folding technique.

2

3a Figure 3a displays a tetrahedron as a force diagram corresponding to a node in equilibrium with two forces upward and two downwards as a form diagram (a node with an anticlastic curvature). This tetrahedron is generated by connecting the end points of the two skew lines $l^{\dagger}_i$ and $l'^{\dagger}_i$. Dividing $l^{\dagger}_i$ and $l'^{\dagger}_i$ into equal segments and establishing a tetrahedron between each two skew segments from each line subdivides the force diagram into multiple tetrahedrons, resulting in a discrete anticlastic surface as a form diagram (Figure 3a-d) (Akbari et al. 2019). Two lines $l^{\dagger}_i$ and $l'^{\dagger}_i$ play the role of subdivision axis in the force and the curvature axis in the form diagram (Figure 3d). These lines are parts of two connectivity graphs, named *labyrinths*, connecting two segregated regions, divided by the anticlastic surface (Fischer and Koch 1989). Using the anticlastic subdivision technique, one can design an anticlastic polyhedral surface, named a Shellular Funicular Structure (SFS). The labyrinths as the subdivision axes in the form and the control handles in the force, facilitate the design process and manipulation of the SFS form-finding technique (Akbari et al. 2020).

Origamizing polyhedral surfaces using tuck-folding

Origami, as an art of folding a flat sheet of material to the desired shape without cutting or stretching, has been investigated for many years. On the other hand, Kirigami is the combination of cuts and folds on a flat sheet of material in order to result in the desired geometry (Castle et al. 2014). Tuck-folding as an origami method can design any freeform surface from flat sheet material by tucking and hiding the unwanted areas of the paper (Tachi 2009). In this process, the Origamizer software can be used to generate the folding/cutting pattern (Demaine and Tachi 2017). The input is a polyhedral mesh and the output is the folding pattern with edge tucking molecules (ETM) and vertex tucking molecules (VTM) added (Figure 4). Each ETM is a quadrilateral with a crease pattern, inserted between a pair of edges in the pattern, corresponding to an edge on the reference mesh (Figure 4). Each VTM is an N-gon surrounded by N edge-tucking molecules (ETM) corresponding to a vertex on the reference mesh. Despite the use of more materials, tuck-folding has many advantages over regular folds. It is easier to fold for complex geometries (especially with anticlastic curvatures) as the fold angle is embedded in the cutting patterns. Furthermore, the ETMs provide extra stiffness and stability to the folds compared to regular folds. This technique includes three steps, cutting to a disk, mapping surface polygons, and generating the crease/cut pattern (Tachi 2009).

- **Cutting to a disk :** To map the surface's polygons to a 2D plane, one needs to construct a polygonal schema, a polyhedral surface homeomorphic to a flat disk that covers the original surface (Figure 4).
- **Mapping the surface's polygons :** Next, the polyhedral mesh is decomposed into individual polygons and isometrically mapped to a 2D plane. In Isometric

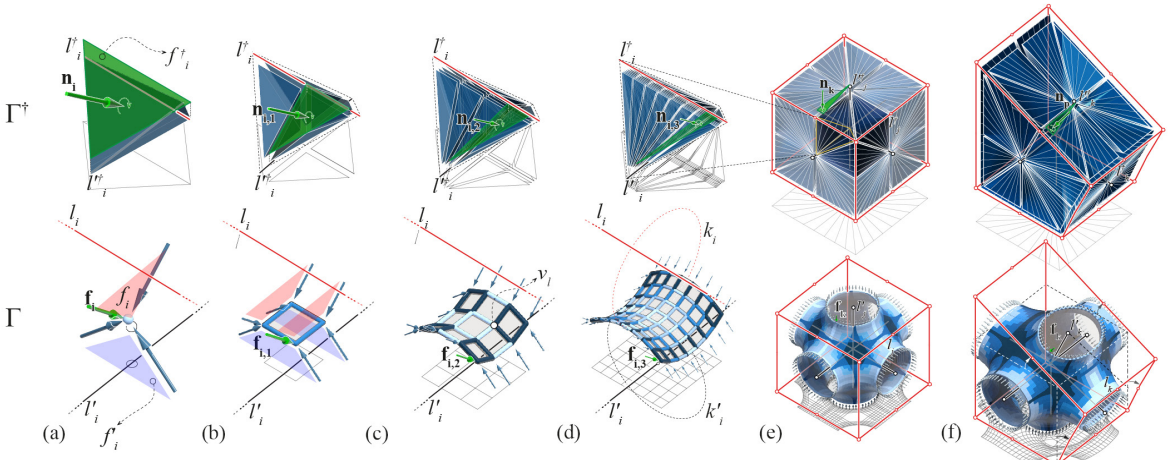

3

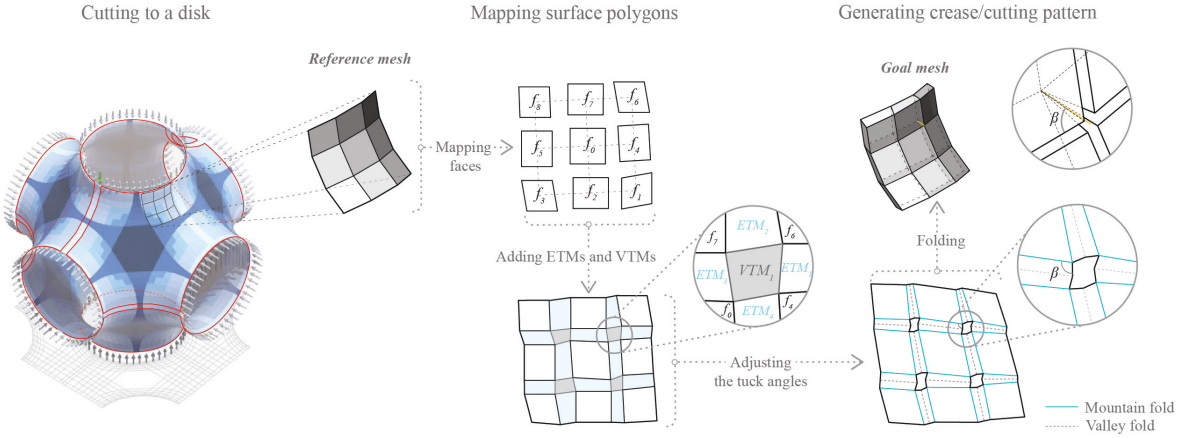

4

mapping, the edge lengths and the polygon's angles will be preserved (Figure 4).

- **Designing the folding/ cutting pattern :** Surface flattening is the problem of generating a 2D pattern from a given 3D shape using an isometric mapping. After adding ETMs and VTMs between the mapped polygons, using specific equality and inequality conditions (Tachi 2009), the method ensures that each ETM is an isosceles trapezoid and eachVTM is a closed convex polygon. By folding a valley crease defined in the middle of each ETM, the ETMs convert to an edge with a hidden tuck in the folding state. Considering the thickness and stiffness of the material, VTMs are cut out as holes, combining the kirigami and origami techniques to facilitate the folding process (Liu et al. 2019). In the goal mesh, the angle between the vertex axis and the edge (i.e., β) is equal to the angle between the VTM's and the ETM's edge (Figure 4). This angle is defined as the tuck angle which assures us that the curvature of the goal mesh in each vertex is equal to the one in the reference mesh.

Problem statement

Although SFSs are considered as efficient structures applicable to different functions in many scales, due to their complex geometry, their process of computational modeling and fabrication are quite challenging, limiting their application in large scales. Furthermore, designing these structures for a predefined boundary condition, control and manipulation of their geometry are not easy tasks. Moreover, fabricating these geometries is mostly possible using additive manufacturing techniques, requiring many supports in the printing process. Recently, Akbari et al. (Akbari et al. 2019, Akbari et al. 2020) proposed different form-finding techniques to design Shellular Funicular Structures in the context of graphic statics based on designing the labyrinths' graphs and applying anticlastic subdivisions in between. But these techniques lack a robust computational algorithm to translate a Cellular (CFS) to a Shellular Funicular Structure (SFS). Furthermore, due to the specific criteria that need to be satisfied in each step, designing the labyrinths' graphs as an intuitive process is not an easy task (Akbari et al. 2020). Moreover, due to their

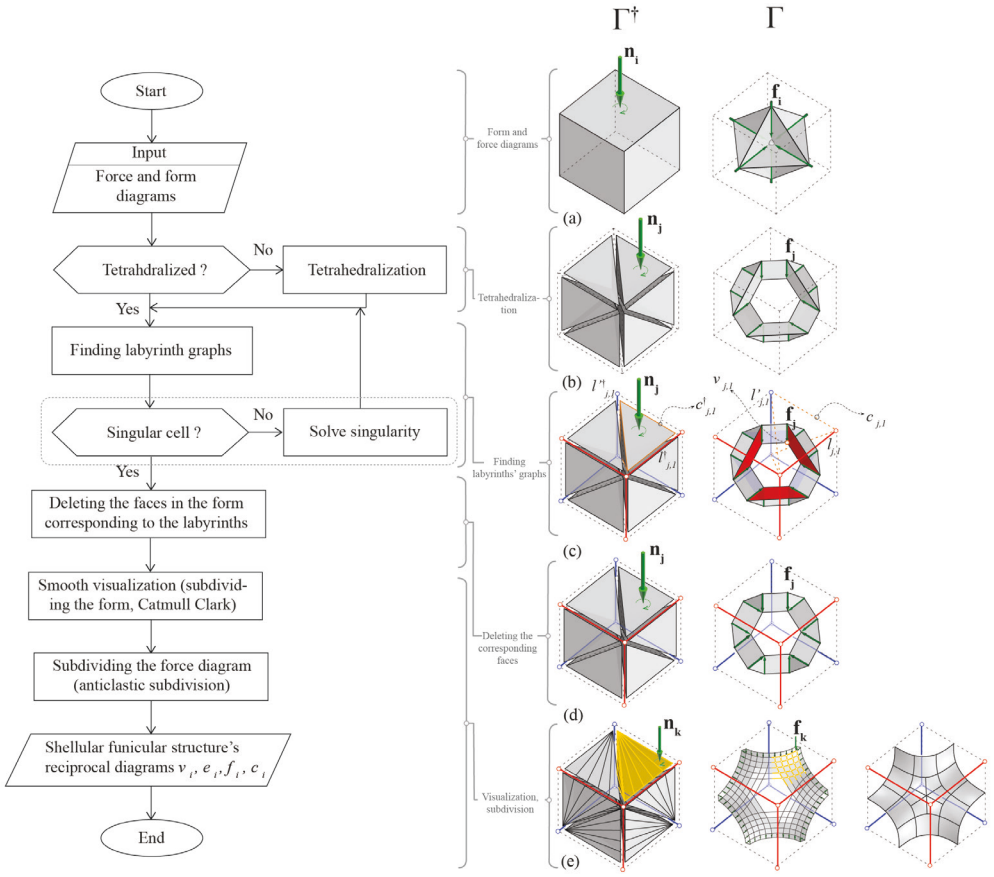

5 The form-finding flowchart (left) and the workflow (right), representing the algorithm for translating a CFS to SFS in the context of graphic statics.

complex interwoven geometry, their fabrication process using digital manufacturing techniques on large scales is challenging. This paper seeks a robust computational method for the design and fabrication of these structures to facilitate their application in macro scales.

Objecives

The main objectives of this paper are to explain a computational algorithm for translating a Cellular Funicular Structure (CFS) to a Shellular Funicular Structure (SFS), and describing a fabrication method to build SFSs out of flat sheets of material using the origami/kirigami technique. As a proof of concept, a structure's geometry with its folding/cutting pattern is designed and fabricated using the SFS and tuck-folding techniques.

METHDOS

The methodology for designing and fabricating SFSs is two-fold. The first section explains the computational algorithm behind the process of translating a CFS to an SFS and the second one describes the fabrication process, inspired by the tuck-folding technique.

Computational design process

To translate the geometry of a Cellular Funicular Structure (CFS) to a Shellular Funicular Structure (SFS), one needs to subdivide the corresponding force diagram, such that each vertex v_i, connected to the group of edges e_i converts to an anticlastic patch, consisting of a group of vertices v_i, faces f_i and edges e_i with smaller lengths, approximating a discrete surface (Figure 3). Materializing the new form diagram by adding faces between the edges (instead of adding thickness to the edges) results in a Shellular Funicular Structure. It is important to notice that the labyrinths l_i and l_i' in the force diagram, overlay on the edges e_i and e_i', corresponding to the faces f_i and f_i' in the form diagram (Figure 3a, b). While materializing the form diagram in the SFS form-finding process, the faces in the form corresponding to the labyrinth edges in the force should not be materialized. Removing these faces results in a 2-manifold geometry (Figure 3).

Although one can use this technique to design an SFS, designing the labyrinths' graphs intuitively is not an easy task. This section describes a computational algorithm for translating a CFS to SFS. The main objective of this algorithm is to find proper three-dimensional labyrinths' graphs

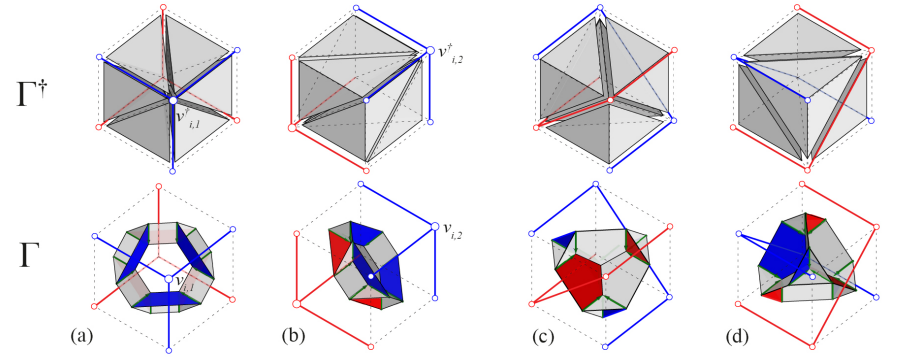

6 Different tetrahedralization of a cube as a force diagram, e.g., into six (a, b) and five (c, d) tetrahedrons, results in different types of the labyrinths' graphs.

7 The process of finding a labyrinths' graph in a tetrahedralized force diagram (a-f) and 3 different types of graphs resulting from this algorithm (g, h, i).

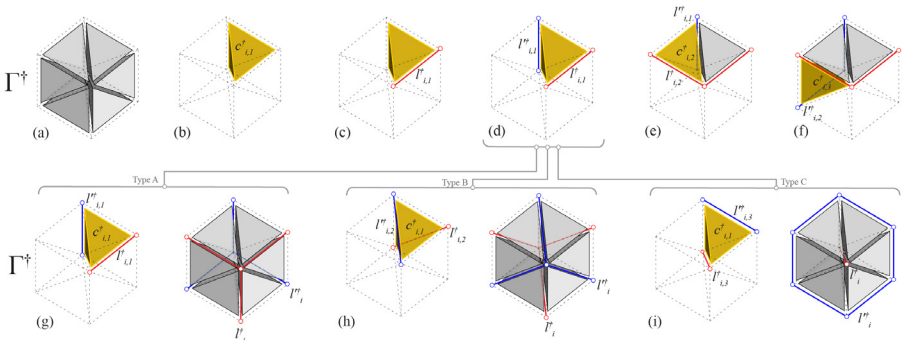

in the form and the force diagrams (inputs) and using them to design the shellular structure (Figure 5). This algorithm receives a form and the force diagram (Figure 5a) that are designed using *Polyframe* (Nejur and Akbarzadeh 2021). After converting the force diagram to a group of tetrahedrons (tetrahedralization, Figure 5b), the algorithm finds the possible labyrinths' graphs in the force diagram (Figure 5c), and remove the corresponding faces to these labyrinths in the form diagram to result in a 2-manifold geometry (Figure 5d). Finally, the smooth version of the form diagram will be visualized using the Catmul-Clark subdivision (Catmul and Clark 1978), and the main shellular load-path will be constructed using the anticlastic subdivision in 3DGS (Figure 5e) (Akbari et al., 2019). In the SFS design process, there are three main principles that need to be considered;

- each pair of labyrinths in the form diagram (e.g., $l_{j,1}$ and $l'_{j,1}$) should form a tetrahedron in between (e.g., $c_{j,1}$), corresponding to an anticlastic node (e.g., $v_{j,1}$) in the form diagram (Figure 5c),
- the force diagram includes two sets of labyrinths ($l^{\dagger}_{j,1}$ and $l'^{\dagger}_{j,1}$) and each tetrahedron in the force diagram (e.g., $c^{\dagger}_{j,1}$), should only include one labyrinth edge from each set which is in a skew position to the other(Figure 5c),
- each labyrinth's edge in the force diagram can be connected to the labyrinth edges from the same set, assuring that the resulting surface (form diagram) will divide the space into two subspaces (Figure 5d, e).

Tetrahedralization

According to the first principle mentioned above, each force diagram should only include tetrahedrons, resulting in 4-valency nodes (nodes that are connected to 4 edges) in the form diagram, representing an anticlastic curvature. The polyhedron tetrahedralization function decomposes a 3D polyhedron into a set of non-overlapping tetrahedra whose vertices are chosen from the vertices of the polyhedron (Toussaint et al. 1993). A convex polyhedron in 3D can always be tetrahedralized without adding new vertices (Steiner points) by connecting any vertex of the polyhedron to all the other vertices (Lennes 1911). Therefore, there might be multiple solutions for tetrahedralizing an input force diagram (Figure 6).

Unfortunately, the minimum-complexity triangulation problem is NP-complete (Below et al. 2000). Hence, in this algorithm, the authors provide part of the possible solutions, using the user's preference (Figure 6). In this process, each input vertex (e.g., $v^{\dagger}_{i,1}$, $v^{\dagger}_{i,2}$) will be connected to all the other vertices in the polyhedron, resulting in a group of tetrahedrons (Figure 6a, b). In some examples like a cube, there might be different techniques resulting in fewer tetrahedrons and new labyrinths' graphs (Figure 6c, d). Since this subject is beyond the scope of this paper, it is going to be studied further in future researches.

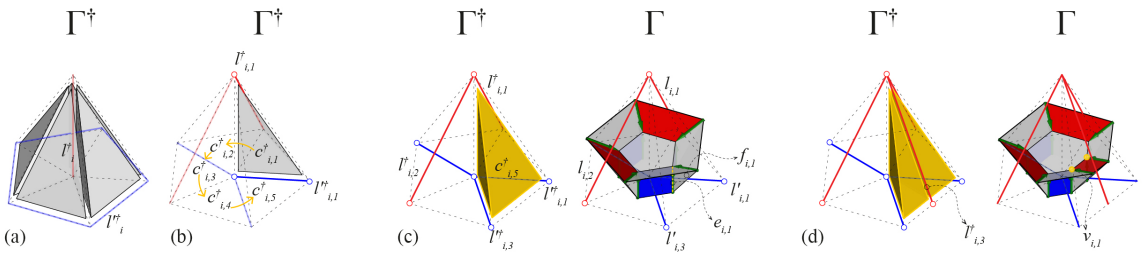

8 A force diagram comprising 5 tetrahedrons (a), an attempt to find the new labyrinths' graphs (b), finding the singular cell (c), and resolving the singularity by subdividing the cell (d).

Finding the labyrinths' graph.

After tetrahedralizing the force diagram, two edges from each tetrahedron, as the labyrinths' graphs' edges, are needed to be selected. Figure 7a-f displays the process for finding the labyrinths' graphs in a cube partitioned into six tetrahedrons, as the force diagram.

This process starts with selecting a random cell $c^{\dagger}_{i,1}$ (Figure 7b). Selecting one of the edges $l^{\dagger}_{i,1}$ of this tetrahedron as a labyrinth's edge (Figure 7c) determines the skew edge $l'^{\dagger}_{i,1}$ as the other labyrinth's edge (Figure 7d). The edges $l'^{\dagger}_{i,1}$ and $l^{\dagger}_{i,1}$ have specific topological relations to each other and are called the dual of each other. The algorithm proceeds through the four neighbors of the tetrahedron cell $c^{\dagger}_{i,1}$. Each neighbor (e.g., $c^{\dagger}_{i,2}$) has a face with three edges and three vertices in common with the previous cell $c^{\dagger}_{i,1}$ (Figure 7e). Among these edges, only one edge is already recognized as a labyrinth edge (i.e., $l^{\dagger}_{i,1}$). If $l'^{\dagger}_{i,1}$ is the dual of $l^{\dagger}_{i,1}$ in cell $c^{\dagger}_{i,1}$, it is the dual of $l^{\dagger}_{i,2}$ in the cell $c^{\dagger}_{i,2}$ as well (Figure 7e). Similarly, the algorithm marches through all the cells in the force diagram and finds the dual labyrinth edges of the previous cell (Figure 7f), until all the cells are passed. In this process, each cell has a pair of labyrinth edges, and the force diagram has two labyrinth graphs $l^{\dagger}_{i}$ and $l'^{\dagger}_{i}$ (Figure 7g).

The resulted labyrinths' graphs are the first type of possible graphs for a force diagram. Since there is a possibility of choosing 3 different pairs of labyrinth edges in a tetrahedron out of 6 edges, choosing different pairs in the first cell $c^{\dagger}_{i,1}$ (Figure 7d) as the labyrinth edges will result in different labyrinths' graphs for the force diagram (Figure 7g, h, i). Hence, according to this algorithm, there are 3 geometrically different labyrinths' graphs for a force diagram.

Singularity

In some situations, due to the specific edge-cell connectivity (when a labyrinth edge is connected to the odd number of cells, e.g., Figure 8a), the algorithm explained above has only one solution (instead of 3). Figure 8a displays a tetrahedralized force diagram with 5 cells and possible labyrinths' graphs $l^{\dagger}_{i}$ and $l'^{\dagger}_{i}$. Figure 8b shows an attempt to find the second pair of the possible graphs. In cell $c^{\dagger}_{i,1}$, two labyrinth edges $l^{\dagger}_{i,1}$ and $l'^{\dagger}_{i,1}$ are selected. After selecting the labyrinths' edges of to the next cells respectively ($c^{\dagger}_{i,2}$, $c^{\dagger}_{i,3}$, $c^{\dagger}_{i,4}$, $c^{\dagger}_{i,5}$), the algorithm faces the cell $c^{\dagger}_{i,5}$ with two edges $l^{\dagger}_{i,1}$ and $l^{\dagger}_{i,3}$ from the same set of labyrinth's graph which is against the main principles of the SFS's technique (Figure 8c). Having two labyrinths in the cell $c^{\dagger}_{i,5}$ will eliminate two neighbor faces of the edge $e_{i,1}$ in the form diagram (faces are marked with blue), resulting in the edge $e_{i,1}$ connected to one face (Figure 8c). In this situation the cell $c^{\dagger}_{i,5}$ is called a singular cell. This issue happens when an edge in the force diagram is connected to an odd number of cells. To solve this issue, one may subdivide the singular cell into two cells and add the new edge as one of the labyrinths' edges (e.g., $l^{\dagger}_{i,3}$) (Figure 8d).

Eliminating the extra faces

Each of the labyrinths' graphs corresponds to a group of faces in the form diagram (Figure 9b, g, l). Eliminating these faces from the form diagram results in a 2-manifold discrete surface (Figure 9c, h, m).

Visualization and subdivision

There are two ways to generate a smooth curved surface from the discrete surface resulted in the previous section. The first solution is to apply a *Catmull-Clark* subdivision, generating a bi-cubic uniform B-spline surface to visualize the smooth anticlastic surface and to compare the geometry of different structures. (Figure 9 d, I, n) (Catmull and Clark 1978). To result in a smooth form diagram in the context of graphic statics, and finding the corresponding load path, one needs to apply the anticlastic subdivision technique (explained in the Introduction) to each tetrahedron cell between each pair of labyrinths (Figure 9 e, j, o). Using this technique, one can intuitively design a Cellular Funicular Structure (CFS) for a specified boundary condition and loading scenario (e.g., a connection, a column, or a bridge) and translate it to its counterpart, a Shellular Funicular Structure (SFS) (Figure 10). It is worth mentioning that in graphical form finding methods, the self-weight of the structure is not considered. To consider the self-weight, one needs to assign mass to each to each node in the system and apply numerical form finding methods (e.g., mass spring or force density) to find the new form in

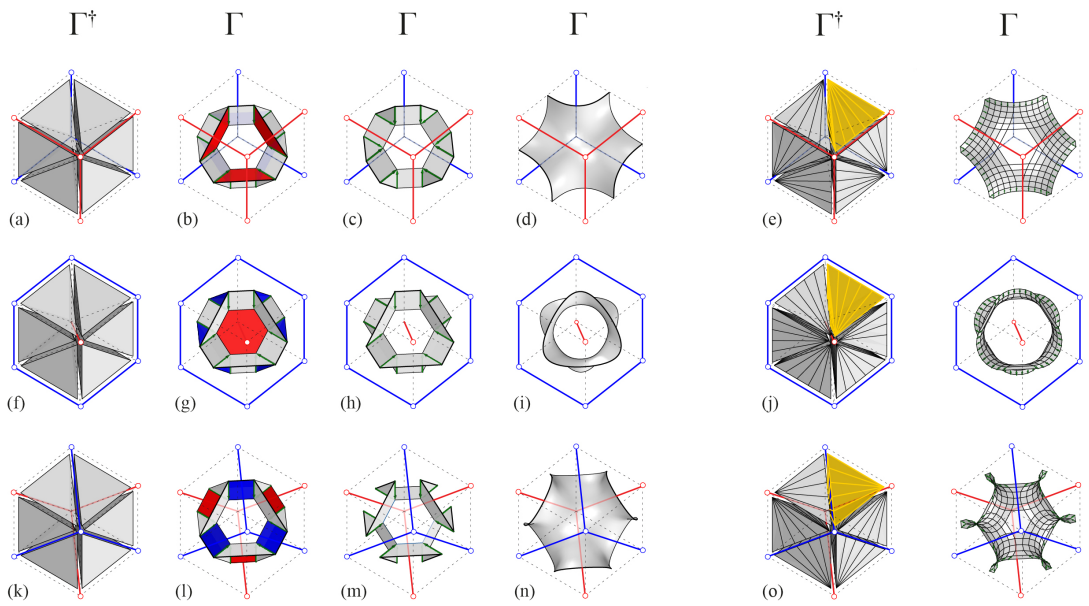

9 Three types of possible labyrinths' graphs for a force diagram (a, f, k) and their reciprocal form diagram with faces correspond to the labyrinths' edges (b, g, l). Removing these faces results in a 2-manifold geometry (c, h, m) which can be converted to a smooth surface by either Catmull-Clark (d, I, n) or anticlastic subdivision in 3DGS (e, j, o).

equilibrium (Adriaenssens et al. 2014).

Fabrication process

Shellular Funicular Structures (SFSs) comprise planar faces resembling a polyhedral surface (Introduction). Therefore, they are a genuine candidate to be fabricated based on Origami/kirigami techniques using flat sheet material. Tuck-folding can be used as a fabrication method to design the folding pattern of these structures. Using this technique, one can either fabricate a shellular system as a discrete single-layer structure, or a double layer formwork for pouring a structural material like concrete (Figure 11a,b). This method finds the folding pattern of a polyhedral surface out of a flat sheet of material, with hidden tucks instead of constructing the exact faces (Figure 11). Furthermore, the edge tucking molecules (ETMs) provide extra stiffness and stability to the folds compared to regular folds. This section explains the process of fabricating a shellular geometry with the tuck-folding method introduced in the introduction (Tachi 2009, Liu et al. 2019).

Fabricating a shellular funicular strture the tuck-folding technique

A shellular geometry with a bounding box dimension of 620mm by 620mm by 310mm as a part of the shellular funicular bridge displayed in Figure 9 is generated using the proposed algorithm for a trial fabrication (Figure 12). This geometry is cut and flattened into 4 cutting patterns, and each pattern has a bounding rectangle dimension of 760mm by 700mm. For the purpose of reducing the shipping cost and the level of folding difficulty, each cutting pattern is further split into 7 smaller parts (Figure 12).

After examining the durability, mechanical properties, and foldability of different materials, 0.5mm stainless steel sheet is selected as the material for fabrication, and an industrial laser cutter is used to cut steel sheets to the target patterns. To mark the fold lines and increase the ease of manual folding, dash line cuts are added to the cutting patterns. The design parameters of the dash line cuts include material density, cutting interval, and dash line width (Figure 13). Material density is defined by the percentage of material left on a folding hinge after dash line cutting; cutting interval means the distance between two neighboring dash line cuts; dash line width indicates the width of the dash line cuts, which confines the bending area along the fold lines. Lower material density, smaller cutting interval, and larger dash line width lead to easier folding, however, small cutting interval also impairs the material strength along the hinges. Based on a series of physical experiments (Figure 15), the cutting interval is determined at 1.5mm. The dash line width has more complex impacts on the folding behavior as too small a width may incur a larger size in the folded geometry, while excessive width increases the folding error. Those parameters are designed in such a way that all folds can be easily achieved by hand, and the dimensions of the folded geometry are as close as possible to the original (Figure 15). To secure the tuck-folding, a pair of circular cuts are also added to each edge tucking molecule which are later aligned and fastened using M3 screws and nuts after folding (Figure 14). When considered as a frictionless hinge and rigid face system, each folding pattern has only one degree of kinematical indeterminacy, meaning that all the folding lines need to be folded at the same time (Figure 16). After folding each part, the shellular

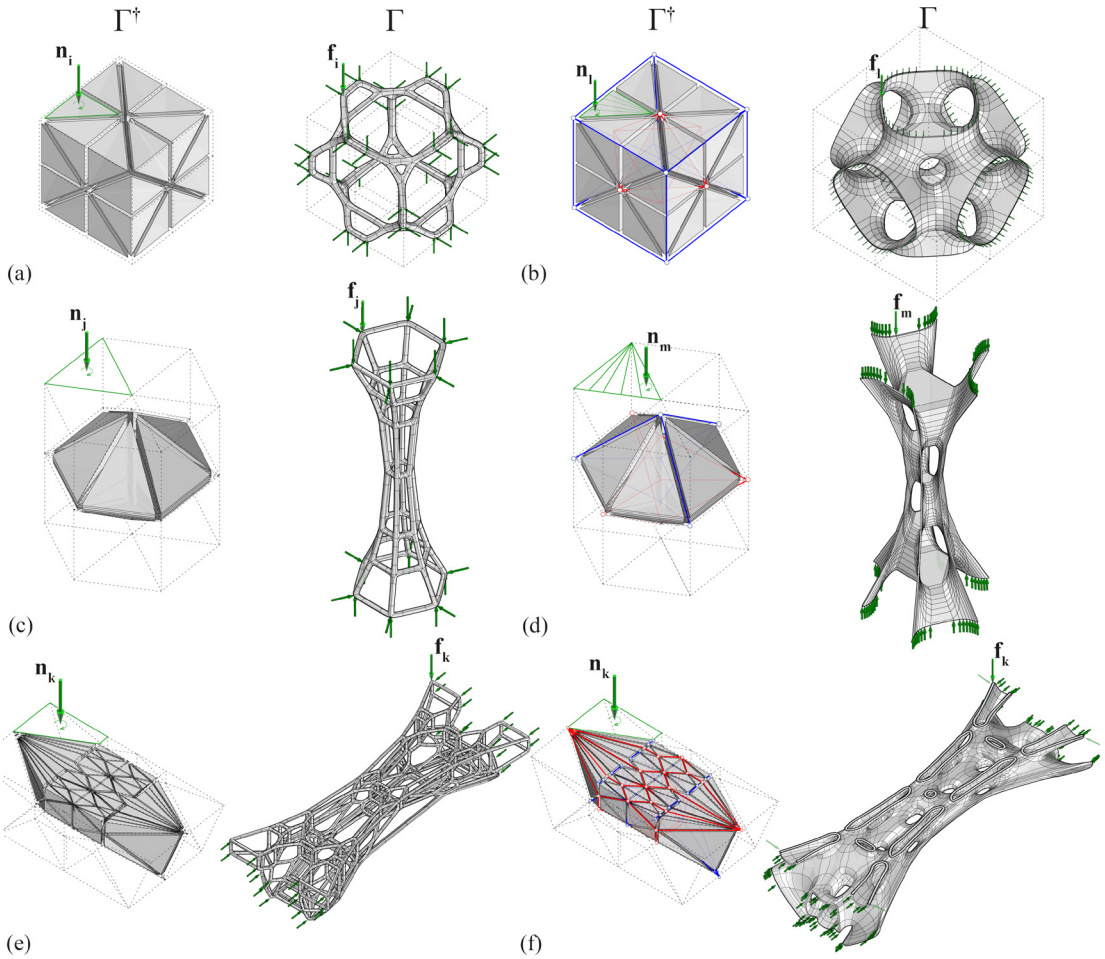

10 The examples of the translation of force and form diagrams of CFSs (a, c, e) to SFSs using the SFS's computational algorithm (b, d, f).

structure is assembled and secured using screws and nuts (Figure 17, 18).

Results and discussion

In this research, the authors proposed a robust computational algorithm to translate a CFS to a SFS. Using this algorithm, one can design any compression/tension-only shellular structure for a defined boundary condition, from meso-scale (e.g., columns and beams) to macro-scale (e.g., a building or a bridge). From the fabrication point of view, due to the interwoven geometry of SFSs which necessitates lots of supports in the printing process, additive manufacturing techniques may not be considered as an efficient process on a large scale. In the meantime, flat sheet materials are an ideal choice because of their accessibility, processibility, low cost, and applicability to large scales. Hence, the second part of the research focused on the fabrication process of SFSs out of flat metal sheets. This method facilitates the use of these structures on the large scale, as a single-layer structure or a double-layer formwork for pouring concrete. (Figure 17, 18). Thanks to the proposed design methodology, the strctures that are designed using this technique can be considered as self-supporting structures, designed for specific loading scenarios. Moreover, adding thickness to the edges of the strucures in the fabrication process results in a stiffer system, increasing the structural capacity of the formwork.

CONCLUSION

Using the proposed technique, shellular funicular structures can be designed and fabricated for macro-scale applications. Future researches include implementing interactive software for the design and manipulation of SFSs and investigating the effect of different tetrahedralization on the results. In the fabrication process, there is a need for improving the process of designing the folding pattern. Controlling the ETMs' widths using the Origamizer software is not an easy task, resulting in a large waste of material. Adding ETMs with different widths to the structure (proportional to the force distribution in the system) results in an efficient system in terms of the material usage with constant stress distribution. It is important to notice

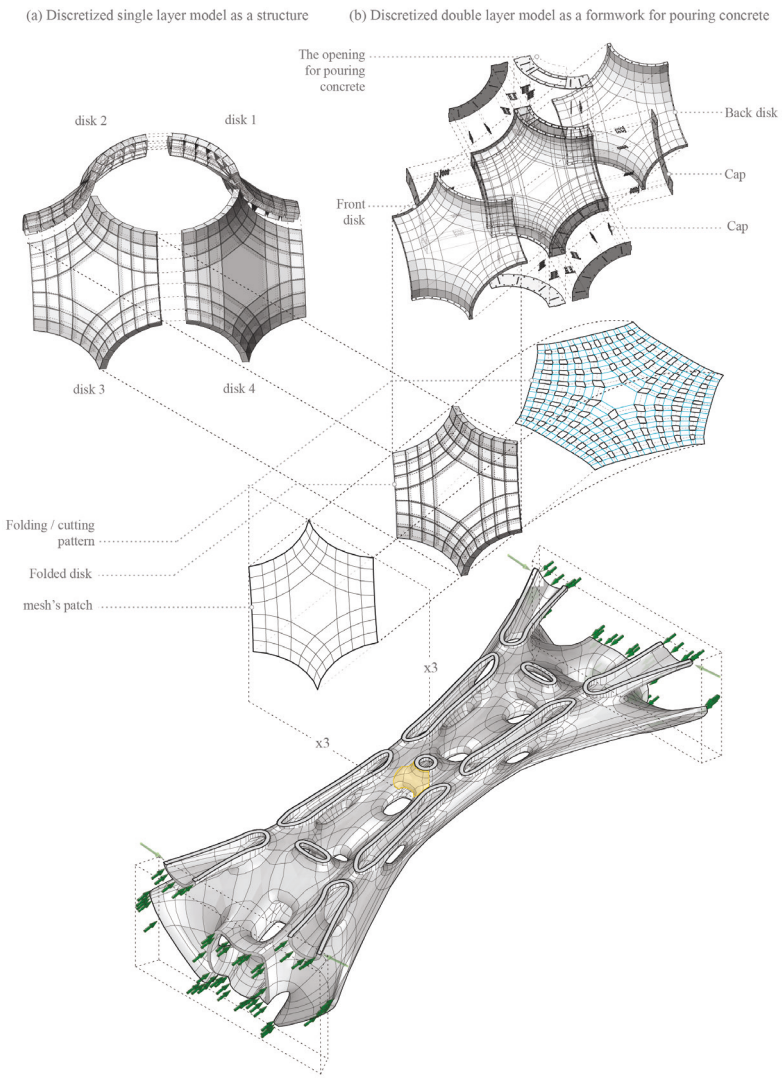

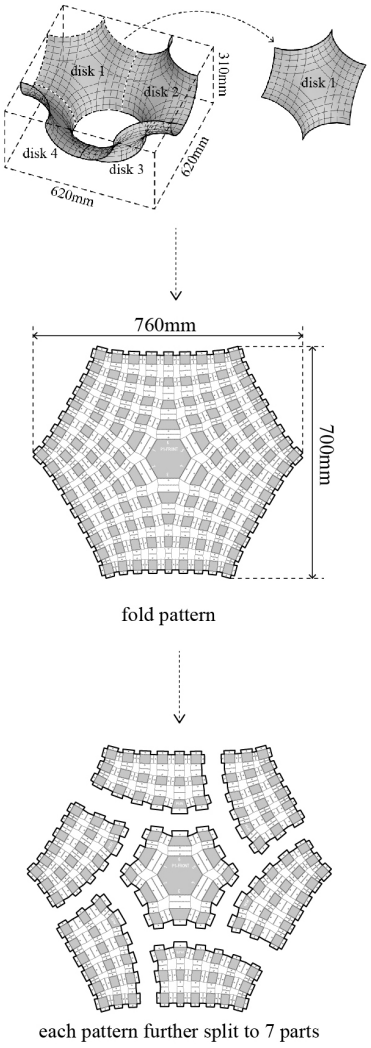

11 12

11 Fabricating an SFS using the tuck-folding technique as a discrete single-layer structure (a), or double-layer form-work for pouring concrete (b).

12 The shellular geometry for trial fabrication and the fold pattern developed using the Origamizer software (Demaine and Tachi

that the structures that are designed using this technique are already in equilibrium for the defined boundary condition and adding non-uniform thickness in the materialization process only yields constant stresses in them.

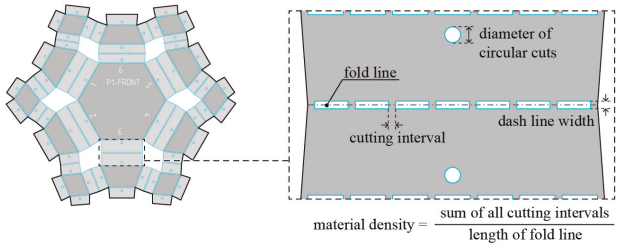

13 The design parameters of dash line cuts.

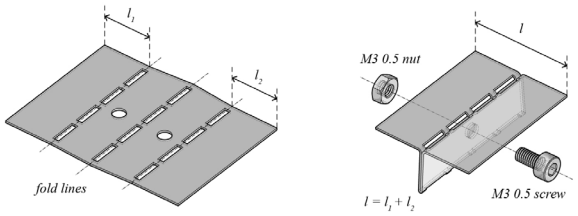

14 Securing the tuck-folding using scews and nuts.

ACKNOWLEDGEMENTS

The authors acknowledge support by National Science Foundation Future Eco Manufacturing Research Grant (NSF, FMRG-CMMI 2037097 and the National Science Foundation CAREER Award (NSF , CAREER-CMMI 1944691) to Dr. Masoud Akbarzadeh. Moreover, the authors are grateful for an inspiring discussion with Dr. Shu Yang from material science department at UPenn.

REFERENCES

[Book] Adriaenssens, S., Block, P., Veenendaal, D. and Williams, C. eds., 2014. Shell structures for architecture: form finding and

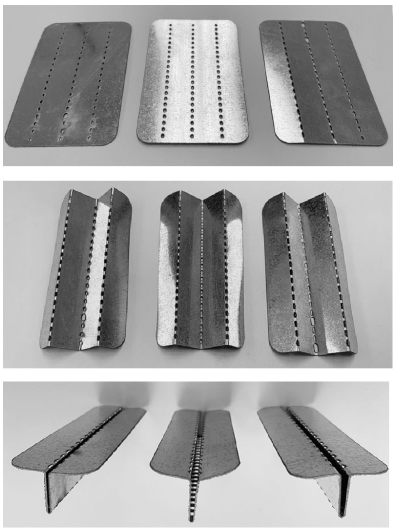

15

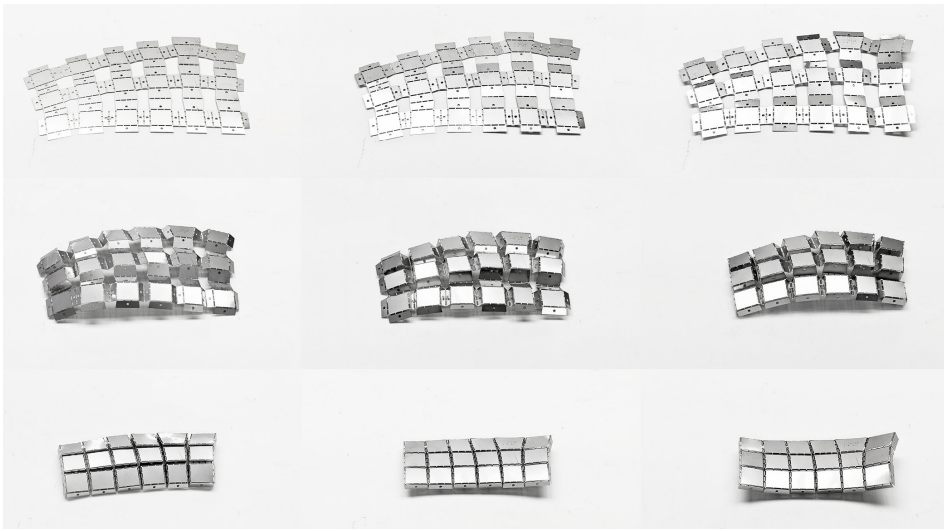

16

15 Folding a stainless steel sheet with different design parameters of dash line cuts.

16 The folding process of a part of the physical model.

optimization. Routledge.

Cremona, L., 1890. Graphical statics: two treatises on the graphical calculus and reciprocal figures in graphical statics. Clarendon Press.

Culmann, K., 1866. Die Graphische Statik, Mayer and Zeller, Zurich.

D. Hilbert, S. Cohn-Vossen, 1990. Geometry and The Imagination, Chelsea Publishing Company, New York, USA.

[Thesis] Akbarzadeh, Masoud. 2016. "3D Graphical Statics Using Reciprocal Polyhedral Diagrams." PhD diss., ETH Zurich.

[Journal Article] Beghini, Lauren L., Juan Carrion, Alessandro Beghini, Arkadiusz Mazurek, and William F. Baker. 2014. "Structural Optimization Using Graphic Statics." Structural and Multidisciplinary Optimization 49.

Catmull, Edwin, and James Clark. 1978. "Recursively generated B-spline surfaces on arbitrary topological meshes." Computer-aided design 10, no. 6: 350-355.

Han, S.C., Choi, J.M., Liu, G. and Kang, K., 2017. A microscopic shell structure with Schwarz's D-surface. Scientific reports, 7(1), pp.1-8.

Han, Seung Chul, Jeong Woo Lee, and Kiju Kang. 2015. "A New Type of Low Density Material: Shellular." Advanced Materials 27 (37): 5506–11.

Lennes, N. J., 1911, "Theorems on the simple finite polygon and polyhedron," American Journal of Mathematics, vol. 33, pp.37-62.
Maxwell, J Clerk. 1864. L. on the calculation of the equilibrium and stiffness of frames. The London, Edinburgh, and Dublin Philosophical Magazine and Journal of Science 27, 182 (1864), 294–299.

McRobie, A., 2016. Maxwell and Rankine reciprocal diagrams via Minkowski sums for two-dimensional and three-dimensional trusses under load. International Journal of Space Structures.

Rankine WJ Macquorn. 1864. XVII. Principle of the equilibrium of polyhedral frames. The London, Edinburgh, and Dublin Philosophical Magazine and Journal of Science.

Tachi, T., 2009. 3D origami design based on tucking molecule. Origami, 4, pp.259-272.

[Conference Paper] Akbarzadeh, M., Bolhassani, M., Tabatabaie, A., Akbari, M., Seyedahmadian, A., Papalexiou, K. and Designs, N. 2021. Saltatur: Node-Based Assembly of Funicular Spatial Concrete. In: Proceedings of the 40th Annual Conference of the Association for Computer-Aided Design in Architecture (ACADIA).

Akbari, Mostafa, Masoud Akbarzadeh, and Mohammad Bolhassani. 2019. "From Polyhedral to Anticlastic Funicular Spatial Structures." In Proceedings of IASS Symposium.

Akbari, Mostafa, Armin Mirabolghasemi, Hamid Akbarzadeh, and Masoud Akbarzadeh. 2020. "Geometry-based structural form-finding to design architected cellular solids." In Symposium on Computational Fabrication, pp. 1-11.

Below, A., De Loera, J.A. and Richter-Gebert, J., 2000, February. Finding minimal triangulations of convex 3-polytopes is NP-hard. In Proceedings of the eleventh annual ACM-SIAM symposium.

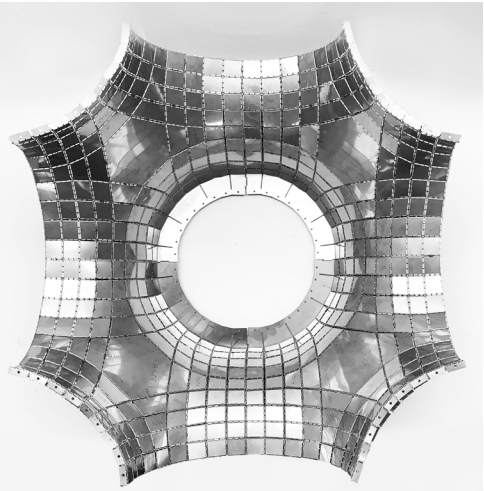

17

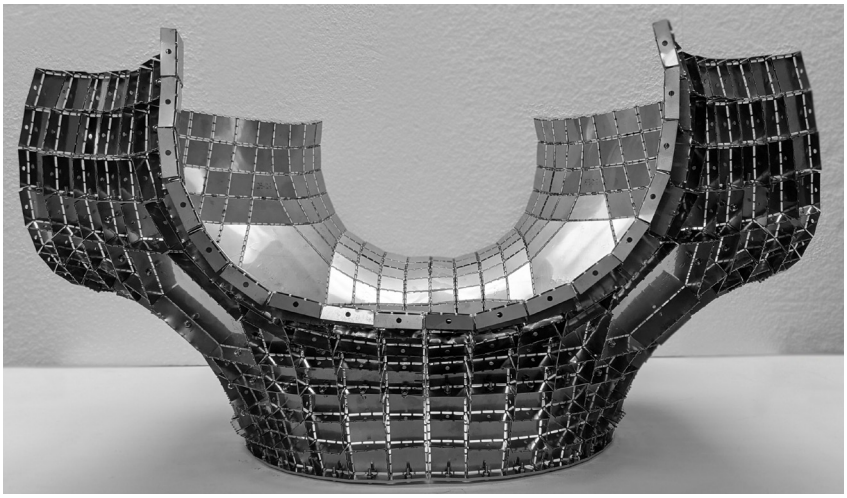

18

17 The final assembled model (top view).

18 The final assembled model (front view).

Canestrini F. Ponte musmeci, 1975.

Castle, T., Cho, Y., Gong, X., Jung, E., Sussman, D.M., Yang, S. and Kamien, R.D., 2014. Making the cut: Lattice kirigami rules. Physical review letters, 113(24), p.245502.

D'acunto, P., Jasienski, J.P., Ohlbrock, P.O. and Fivet, C., 2017. Vector-based 3d graphic statics: transformations of force diagrams. In Proceedings of IASS Annual Symposia.

Demaine, E.D. and Tachi, T., 2017. Origamizer: A practical algorithm for folding any polyhedron. In 33rd International Symposium on Computational Geometry (SoCG 2017). Schloss Dagstuhl-Leibniz-Zentrum fuer Informatik.

Konstantatou, M. and Mcrobie, A., 2017, September. 3D Graphic statics and graphic kinematics for spatial structures. In Proceedings of IASS Annual Symposia (Vol. 2017, No. 12, pp. 1-10). International Association for Shell and Spatial Structures (IASS).

Liu, J., Chuang, G., Sang, H.C. and Sabin, J.E., 2019, August. Programmable Kirigami: Cutting and Folding in Science, Technology and Architecture. In International Design Engineering Technical Conferences and Computers and Information.

Meeks III, W. and Pérez, J., 2011. The classical theory of minimal surfaces. Bulletin of the American Mathematical Society, 48(3), pp.325-407.

Nejur, A. and Akbarzadeh, M., 2021. PolyFrame, Efficient Computation for 3D Graphic Statics. Computer-Aided Design, 134, p.103003.

Otto, Frei, 1970, "Soap bubble experimentation", The institute for lightweight structures, University of Stuttgart.

Tango, Alba Fermoso. "Equilibrio." sumaunahoramenos. 2012. http://sumaunahoramenos.blogspot.com/2012/07/equilibrio.html.

Toussaint, G.T., Verbrugge, C., Wang, C. and Zhu, B., 1993. Tetrahedralization of simple and non-simple polyhedra. In Proc. 5th Canadian Conference on Computational Geometry.

Vlahinos M. and O'Hara R., nTopology, 2020, https://www.aero-spacemanufacturinganddesign.com/.

IMAGE CREDITS

Figure 1: image cedits are listed in the caption.
All other drawings and images by the authors.

Mostafa Akbari is a Ph.D. student at the Polyhedral Structures Laboratory, Weitzman School of Design, University of Pennsylvania, specializing in computational design and advanced manufacturing. His main research topic is Shellular Funicular Structures, a novel geometrical form finding method to approximate the geometry of minimal surface structures in the context of graphic statics.

Yao Lu is a Ph.D. student at the Polyhedral Structures Laboratory, Weitzman School of Design, University of Pennsylvania. He is a design researcher with a great interest in generative design, robotic fabrication, 3D printing, and computer graphics.

Masoud Akbarzadeh is a designer with a unique academic background and experience in architectural design, computation, and structural engineering. He is an Assistant Professor of Architecture in Structures and Advanced Technologies and the Director of the Polyhedral Structures Laboratory (PSL) at the University of Pennsylvania.